This is a repository copy of *Fuzzy set-based methodology for manufacturing parameter determination of 3D-printed polylactide components with user-specified strength, geometrical design, and cost requirements*.

White Rose Research Online URL for this paper:
https://eprints.whiterose.ac.uk/198267/

Version: Published Version

Article:

ORIGINAL ARTICLE

Fuzzy set-based methodology for manufacturing parameter determination of 3D-printed polylactide components with user-specified strength, geometrical design, and cost requirements

Ruixuan Tu[1] | Inna Gitman[2] | Luca Susmel[3] (ID)

[1]Department of Mechanical Engineering, University of Sheffield, Sheffield, UK

[2]Department of Mechanics of Solids, Surfaces & Systems, University of Twente, Enschede, The Netherlands

[3]Department of Civil and Structural Engineering, University of Sheffield, Sheffield, UK

Correspondence
Ruixuan Tu, Department of Mechanical Engineering, University of Sheffield, Sheffield, UK.
Email: rtu1@sheffield.ac.uk

Abstract

A computational data-driven fuzzy set-based methodology is proposed and applied to determine, with high accuracy, the manufacturing parameters of 3D-printed polylactide (PLA) components, ensuring user-specified failure tensile strength and design requirements (here: the notch root radius). Hence, the novel decision-making tool to estimate 3D-printing process parameters is offered, ensuring desired design characteristics and the mechanical performance. The estimated manufacturing angle and infill density have been adjusted to provide meaningful values for real applications, still resulting in accurate predictions through the validation process. Following the success of these design and strength driven estimations, an extension of the proposed methodology to the cost-saving problem has then been suggested by introducing printing period and material cost as extra inputs to the decision-making process.

KEYWORDS
3D-printing, cost control, estimation accuracy, failure strength, fuzzy inference system

Highlights

- Technical parameters of 3D-printed PLA are estimated, using fuzzy inference system.
- Estimations are optimized, ensuring user-specified geometrical and strength parameters.
- Cost-control parameters are included together with geometrical and strength parameters.
- Accuracy of the proposed approach is checked through a devised validation test.

1 | INTRODUCTION

Rapid prototyping, also known as additive manufacturing or 3D-printing, has brought a remarkable digital revolution to the manufacturing industry in the last decades. Compared with the conventional subtractive manufacturing process such as machining, milling, and shaping, parts are additively built layer by layer in 3D-printing, allowing more flexibility and area of applications. For example, 3D-printing has been widely used in tissue engineering for fabricating artificial tissue constructs with solid[1,2] and hollow[3,4] structures due to its high accuracy in vitro models.[5] Additionally, during the 2020 pandemic, 3D-printing was successfully used (based on the open-source design data) to manufacture in-house, on-demand face shields to be used as extra personal protective equipment (PPE).[6] Recent research has also demonstrated that laser sintering-3D-printed body armor can achieve stab protection to UK body armor standards, due to the high degree of design freedom provided by 3D-printing.[7]

As a branch of the giant 3D-printing family, fused deposition modeling (FDM) is one of the most common AM technologies based on material extrusion by depositing melted materials selectively on the printing platform layer by layer. The most commonly used materials in FDM are polymers, such as polylactide (PLA), as thermoplastic materials can be easily melted and extruded from the nozzle of a 3D-printer. The path of the nozzle is generated based on the layer geometry which is the outcome of the part being sliced into super-thin layers with the help of computer-aided-design (CAD) software packages.[8] Upon cooling on the printing platform, layers of thermoplastic materials bond together and eventually form a three-dimensional part as designed.

Generally, aiming at material and time saving, the internal structure of a printed object can be partly hollow where the amount of material-filled volume is defined as the infill density. Infill density is found to significantly affect the weight,[9] strength,[10] stiffness,[11] and printing time[12] of the printed part. In addition, various types of infill pattern (internal shape of a part) have been reported to cause different levels of anisotropy,[13] which leads to significant mechanical performance variance.[14,15] As such, if the 3D-printed part has to comply with specified mechanical requirements, it is vital to take into account the infill density.

In addition to the infill density, the mechanical behavior of printed objects with FDM can be influenced by multiple processing parameters, including temperatures of nozzle and printing plate, layer thickness, printing speed, feed rate, and printing direction.[16,17] Printing direction, which has recently raised increasing interests of the international research community, is seen to have a significant influence on the mechanical response of common FDM materials, such as PLA. The change in printing direction has been shown to cause anisotropic behavior which is one of the main characteristics of 3D-printing.[18] It has been suggested that anisotropy plays a role of primary importance, as far as the mechanical response of 3D-printed object is concerned.[19,20] This is also seen in experiments where three different printing orientations (perpendicularly, on-edge and flat) cause variations in both strength performance and fracture behavior.[21,22] Furthermore, when it comes to objects printed flat on the build plate, the mechanical behavior depends on the manufacturing raster angle.[19,23,24] This is because, by changing the manufacturing raster angle, the strength performance of the printed objects vary based on the average layer adhesion and the ultimate tensile strength of the 3D-printed material.[25,26] Specifically, Weake et al.[27] found that the tensile strength of an acrylonitrile butadiene styrene (ABS) part could be up to 150% higher when the applied force is parallel to the material filaments (manufacturing angle equals to 0°) than perpendicular (manufacturing angle equals to 90°). In the former case, the overall strength is related to the axial strength of each material filament, whereas in the latter case, the overall strength only depends on the bonding forces between adjacent filaments.[19] Thus, by comparing the average layer adhesion[25] and the ultimate tensile strength of the material,[24] it is identified that parallel loading leads to larger overall tensile strength than perpendicular loading. As such, manufacturing angle is definitely worth of extra attention as far as the mechanical performance of a 3D-printed object is concerned.

It has been seen in numerous experimental studies that both infill density and manufacturing angle can influence simultaneously the mechanical behavior of 3D-printed objects. Although the individual effect of these parameters was analyzed,[27,28] due to the complexity of the cross-correlations between them, the estimation of the mechanical strength can be highly inaccurate where both infill density and manufacturing angle vary. The determination of the mechanical behavior of a 3D-printed part still relies on either numerous tests or empirical relations which are in any case the outcome from comprehensive experimental investigations. Hence, it has become a priority to provide an alternative methodology requiring fewer experimental tests for formulating the relationship between the mechanical behavior of a 3D-printed object and multiple manufacturing parameters.

Data-driven solution has shown its capability of overcoming the above difficulties by gaining knowledge and recognizing and creating patterns among the data

—WILEY—

directly. Typical data-driven methods, including artificial neural networks (ANN), fuzzy inference system (FIS), and other techniques, are widely applied to study the mechanical behavior of 3D-printed object.[27,29] The complexity caused by the joint effect of multiple parameters is seen to be effectively solved by the application of non-linear regression solutions included in the aforementioned techniques.[26] Specifically, compared with ANN—a "black box" structure, FIS framework has a "grey box" structure which benefits from its fuzzy rules, allowing more user control through the relatively transparent structure. Apart from the user-friendly characteristic of FIS, ease to use and less required data make FIS a highly welcome data-driven solution in scientific community. Considering the error that always exists in manufacturing and testing 3D-printed components, FIS is an appropriate method for this application due to its tolerance of data imprecision.[30]

Previous studies have proven that FIS has the capability to estimate the tensile strength with given manufacturing and geometrical parameters.[26] However, the current industrial problem is that with both strength and geometrical design requirements set for a 3D-printed object, the optimal combination of manufacturing parameters can be impossible to be determined a priori. Therefore, in this paper, attempts have been made to solve such a problem by estimating manufacturing angle and infill density with the provided requirement of strength and geometry. Besides, adjustments are conducted to identify the most appropriate combination of both manufacturing parameters in order to meet specific industrial needs, for example, setting material-saving as a top priority. Due to the fact that the estimation in the present work seeks for manufacturing parameters which lead to required strength and geometry, it will be referred to as *inverse estimation* in the following sections, contrary to *direct estimation*, resulting in strength based on the given manufacturing parameters reported in our previous work.[26]

In Section 2, the design and manufacturing of tested components will be introduced. Then, in Section 3, the classification of experimental data will be explained, followed by the construction of FIS. Adjustments and analysis of estimation results as well as the validation process will be illustrated in the same section. Section 4 will introduce an extra case study where cost related variables are included.

2 | MANUFACTURING OF SPECIMENS

3D-printed specimens used in the present research were manufactured with 3D-printer Ultimaker 2 Extended+,

using 2.85-mm-diameter PLA filaments. The manufacturing parameters were set as shown in Table 1. All specimens were tested with a Shimadzu universal axial machine where the displacement rate was equal to 2 mm/min.[31]

The drawings seen in Figure 1A include the dimensions of all specimens used in the present investigation with different geometrical characteristics. Figure 1B shows the definition of the manufacturing angle being adopted, which refers to the angle between the longitudinal axis of the specimen and the positive *y*-axis of the building plate. The particular choice of geometries (notched specimens in Figure 1A) was used to support the extensive testing of FIS methodology discussed in our previous investigation.[26]

3 | INVERSE ESTIMATION USING FIS

A FIS is based on the idea of fuzzy sets which was first proposed by Zadeh[32] in 1965. The system can be used to

TABLE 1 Predetermined manufacturing parameters for 3D-printing process.[31]

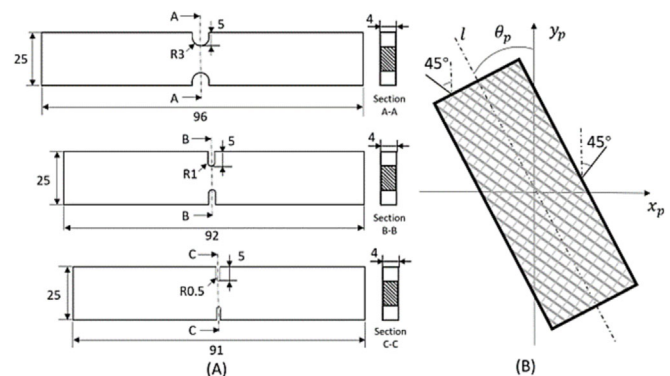| Manufacturing parameters	Values/selections
Layer height	0.1 mm
Shell thickness	0.4 mm
Infill pattern	Grid
Build-plate temperature	60°C
Printing speed	30 mm/s
Nozzle size	0.4 mm
Nozzle temperature	240°C

FIGURE 1 (A) Technical drawings of 3D-printed specimens with three different dimensions and (B) manufacturing angle between the longitudinal axis and the main printing direction.[31] [Colour figure can be viewed at wileyonlinelibrary.com]

model complicated problems with nonlinearities in a way similar to human reasoning process. Particularly in engineering applications, fuzzy sets theory aims at efficient computational methods that tolerate suboptimality and imprecision.[33]

In traditional dual logic, a statement has to be either true or false (nothing in between). In the theory of sets, an element can either belong to a set or not.[34] However, in the theory of fuzzy sets, the truth of any statement becomes a matter of degree[35] (degree of membership), which helps formulate the mapping from a given input to an output. Such mapping can be formulated by a group of IF–THEN rules which are extracted from the historical data and the formulation is normally considered as the "training" stage of a FIS.[36] With new input data provided, the trained FIS can provide an estimation of the unknown output. In the present investigation, the input refers to manufacturing and geometrical design parameters and the output refers to the failure tensile strength of 3D-printed parts. For readers' easier understanding, the fundamentals and calculations of FIS will be presented in Sections 3.3 and 3.4 with a simplified example.

3.1 | Inverse problem setup

Before stepping into the fundamentals of FIS, it is important to first identify the engineering problem. As mentioned in Section 1, generally, the goal of an industrial process is to find the optimal solution of manufacturing parameters that ensures predetermined values of strength and geometry. Owing to the success of FIS in the previously investigated direct estimation (from manufacturing parameters to strength),[26] the new input of the inverse FIS in the present investigation is set to be strength and geometrical parameters, that is, tensile strength and notch root radius. Hence, the manufacturing angle and the infill density have become the output of this new inverse estimation.

3.2 | Experimental data and classification

After the inverse problem has been set up, the introduction of experimental data for training and validating FIS is also of great importance. The experimental data are originally adopted from Ahmed and Susmel[31] and reported in Table 2 where every value of the reported failure strength was calculated by averaging 3.[26] Therefore,

there are 27 experimental data sets, each of which has a unique combination of four parameters. Relevant parameters in Table 2 are referred to as radius—notch root radius (mm), σ_f—failure tensile strength (MPa), θ_p—manufacturing angle (°), infill density (%).

To show the reliability of the FIS methodology, it is necessary to have not only enough data for defining the fuzzy rules but also a group of data needed exclusively for validation. In this paper, a new classification principle is adopted where all specimens with radius equal to 1 mm are treated as *unknown* data and classified as the validation group. This is to evaluate the performance of FIS to deal with the *unseen* value—that is, how well FIS will deal with the unseen data with notch root radius equal to 1 mm if the system has only seen data with 0.5 and 3 mm.

3.3 | Sugeno FIS

It is seen that both output parameters in Table 2, the manufacturing angle and the infill density, have crisp values—measurable, precise numbers/values; in other words, these characteristics are members of classic, rather than fuzzy set with a degree of membership description. Hence, the Sugeno FIS[37] is selected as it is relatively more efficient to model the nonlinear relationship between crisp values. Different from Mamdani FIS[38] adopted in the past work,[26] Sugeno FIS allows the output membership function (MF) to be a constant or a linear function of input values. It is more suitable for the current research than Mamdani FIS as the latter has a requirement of transforming crisp output values into MFs, which could generate further numerical error if the parameters of MFs are not set to optimal. Besides, compared with Mamdani FIS, Sugeno FIS has the advantage of computational efficiency since the calculation in defuzzification process refers to the weighted average of multiple data (illustrated in following paragraphs and Figure 2), rather than the centroid solution in Mamdani FIS which has been previously introduced.[20,21,26]

Being in itself a recap of the FIS, the general stages of setting up a Sugeno FIS are illustrated as follows. In the beginning, a group of "training data" is fed to formulate the fuzzy rule base which builds mappings between existing input and output. In order to make predictions of a new unknown output, the new known input data have to be first fuzzified into a membership value using MF. One of the typical MFs is triangular MF[39] as shown in Equation (1), which is popular due to its simplicity and quick response:

TABLE 2 Summary of experimental data for testing U-notched specimens.

Specimen	Input		Output	
	Radius (mm)	σ_f (MPa)	θ_p (°)	Infill density (%)
1	0.5	9.7	0	30
2	1	9.5	0	30
3	3	10.9	0	30
4	0.5	13.1	0	50
5	1	13.8	0	50
6	3	14.4	0	50
7	0.5	17.4	0	70
8	1	16.9	0	70
9	3	18.6	0	70
10	0.5	8.2	30	30
11	1	8.5	30	30
12	3	10.0	30	30
13	0.5	11.5	30	50
14	1	12.0	30	50
15	3	12.5	30	50
16	0.5	12.2	30	70
17	1	11.9	30	70
18	3	13.9	30	70
19	0.5	8.0	45	30
20	1	8.1	45	30
21	3	9.8	45	30
22	0.5	11.0	45	50
23	1	11.9	45	50
24	3	13.5	45	50
25	0.5	15.1	45	70
26	1	15.2	45	70
27	3	16.4	45	70

FIGURE 2 Decomposition of a Sugeno fuzzy inference system. [Colour figure can be viewed at wileyonlinelibrary.com]
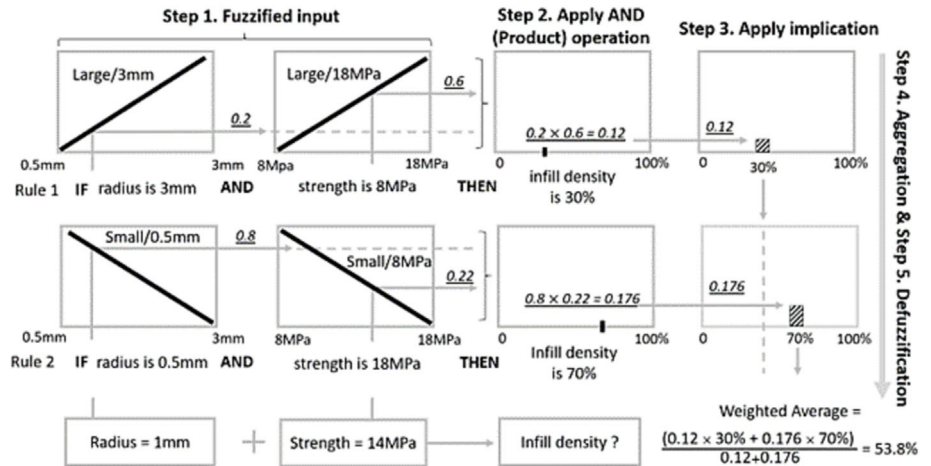
$$\mu(x) = \begin{cases} 0, & x \le a, \\ \dfrac{x-a}{b-a}, & a < x \le b, \\ \dfrac{c-x}{c-b}, & b < x < c, \\ 0, & x \ge c, \end{cases} \quad (1)$$

where a, b, and c are parameters of the function defined by users and $\mu(x)$ is the membership value of the corresponding input x. For various fuzzy rules, parameters of the MF could be different so the fuzzification of a FIS which contains several rules has a parallel data processing pattern. Note here these fuzzy rules have only helped on generating parameters of MF while they have not interfered with input data yet.

Note that the triangular MF is used both in the following explanatory example in Section 3.4 and in the estimation process for the general experimental data. Moreover, with the focus of the current research being applying the FIS methodology for the inverse estimation of 3D-printing technical parameters, the effect of various types of MF will not be detailed in this content. However, the triangular MF is reported to have a top-tier performance, compared with other MFs.[40,41]

The derived membership values are then brought to the fuzzy inference engine, which contains a group of fuzzy calculus that can process the membership value with respect to fuzzy rules. The detailed calculus will be introduced in the later section, together with an illustrative example. The output of a Sugeno fuzzy inference engine is a combination of two values—m_i and n_i where m_i refers to the processed membership value of the new input for ith fuzzy rule and n_i refers to the known output value (from training data) for the same rule.

As mentioned previously, the Sugeno FIS does not include any MF calculation in the output stage apart from a weighted average calculation as shown below:

$$W_a = \frac{\sum_{1}^{k} m_i * n_i}{\sum_{1}^{k} m_i}, \quad (2)$$

where k refers to the total amount of fuzzy rules and W_a refers to the calculated weighted average value. Eventually, the value of W_a is the estimated output value for the new input.

3.4 | Sugeno FIS with an illustrative example

Since the general stages of constructing a Sugeno FIS have been introduced, it is possible now to illustrate the detailed calculation with a synthetic example. Figure 2 shows the decomposition of a Sugeno FIS calculation for some fabricated data. Note that in Figure 2, the calculation and setup of MF for input parameters have been partly simplified, aimed at helping the readers to better understand.

The process starts from the definition of two fuzzy rules, formulated based on the existing experimental data, which in the linguistic form are as follows:

Rule 1. "if radius is 3 mm and strength is 10 MPa, then infill density will be 30%";
Rule 2. "if radius is 0.5 mm and strength is 18 MPa, then infill density will be 70%."

As the next step, input parameters are fuzzified using triangular MFs, resulting in membership values. For the first parameter of synthetic data, radius ranges from 0.5 to 3 mm, and the membership value ranges from 0 to 1. Therefore, MFs for the radius (the first column from left in Figure 2) can be calculated using Equation (3):

$$\mu(x) = \begin{cases} \dfrac{x-0.5}{3-0.5}, & \text{if radius is large (Rule 1),} \\ \dfrac{3-x}{3-0.5}, & \text{if radius is small (Rule 2).} \end{cases} \quad (3)$$

With a new radius value equal to 1 ($x = 1$) as input, the corresponding membership value of both rules can be found as $\frac{1-0.5}{3-0.5} = 0.2$ and $\frac{3-1}{3-0.5} = 0.8$ based on Equation (3). Similarly, membership values, $\frac{14-8}{18-8} = 0.6$ and $\frac{18-14}{18-8} = 0.4$, can be obtained for the second parameter—strength (the second column in Figure 2).

Then, the next step, the AND operation, mentioned in both rules above, refers to as implication: for example, for 30% infill density (consequent of Rule 1), the outcome of this implication stage is a membership value (the product of radius and strength membership values) $0.2 \times 0.6 = 0.12$. Therefore, combined with the 30% infill density, the calculation result for the first row is 0.12/30% (0.12 for the calculated membership value and 30% for the consequent value). Similarly, the calculation result for the second row is 0.176/70%, where 0.176 is obtained from $0.8 \times 0.22 = 0.176$.

Exercising all existing rules (two in our case), the weighted average of all outcomes is calculated as shown in Figure 2, resulting in the estimated infill density. Hence, in our illustrative example, with knowing data

from Rules 1 and 2, the estimated infill density for a new specimen (with "notch root radius—1 mm and tensile strength—14 MPa") is $\frac{0.12\times30\%+0.176\times70\%}{0.12+0.176} = 53.8\%$. Note that MFs of output parameters are now in form of constants rather than functions thanks to Sugeno FIS.

3.5 | Estimation results and adjustments

Returning back to the original experimental data reported in Table 2, a new FIS can be constructed from all *known* (unshaded) specimens, following the procedure introduced in Section 3.5. Then, the new *unknown* (shaded in Table 2) data from the validation group is fed into the system and the estimation result based on the validation group is noted in Table 3. The "experiment output" in Table 3 includes actual values of manufacturing angles and infill densities repeated from Table 2; they are eventually compared with "estimation output."

Since the outcome of this inverse FIS is values of manufacturing parameters which are to be fed into 3D-printers, it is very likely that the estimation results will be correct mathematically, but the values are somewhat meaningless to the printer due to possible printer specifications. Hence, the adjustments of results based on real applications (taking particular specifications of a 3D-printer into account) are necessary in order to avoid meaningless values. To take an example of the adjustment of manufacturing angle, which follows the principle of "proximity," if two estimated manufacturing angles are 4.3° and 12.9° for two different specimens, the adjusted estimation result will be 0° and 15°, respectively. Similarly, for infill density, if two estimated infill densities are 67.6% and 61.4% for two different specimens, the adjusted estimation result will be 70% and 60%, respectively. Both adjusted estimation results have been included in Table 3, in "adjusted estimation" column.

3.6 | Estimation error calculation

In order to evaluate the accuracy of the proposed inverse FIS methodology, estimated outputs (P_{est}) are compared with the actual experimental outputs (P_{exp}), see Table 3, where the *absolute* error is calculated according to this simple definition:

$$Error = \left| P_{est} - P_{exp} \right|, \tag{4}$$

as the presence of "0" in the actual experimental manufacturing angle (and hence in a denominator for the case of relative error calculations) could cause numerical issues.

As to the analyzing errors presented in Table 3, it is interesting to note a high estimation error for manufacturing angle of Specimen 5 (see 30° absolute error). We attempted to analyze this relatively high value and came up with the following explanations:

- the two adjacent rules influencing the estimation of Specimen 5 are Specimens 18 and 24 (see Table 2), since the strength of Specimen 5, which is 13.8 MPa, lies in between 13.5 (Specimen 24) and 13.9 MPa (Specimen 18);
- infill densities are also relatively close to each other (identical in Specimens 5 and 24);

TABLE 3 Experimental output together with the estimation output and its corresponding adjustment.

Specimen	Experiment output		Estimation output		Adjusted estimation		Absolute error	
	θ_p (°)	Infill (%)	θ_p (°)	Infill (%)	θ_p (°)	Infill (%)	Error θ_p (°)	Error infill (%)
2	0	30	5.3	30	0	30	0	0
5	0	50	33.7	60	30	60	30	10
8	0	70	9	70	15	70	15	0
11	30	30	24.1	30	30	30	0	0
14	30	50	30	64.3	30	60	0	10
17	30	70	30	61.4	30	60	0	10
20	45	30	37.5	30	30	30	15	0
23	45	50	30	61.4	30	60	15	10
26	45	70	45	70	45	70	0	0
					Average error		8.3	4.4

Note: The absolute error between the experimental output and the adjusted estimation.

- therefore, intuitively, the estimated manufacturing angle of Specimen 5 should lie somewhere between 30° (Specimen 18) and 45° (Specimen 24).

Moreover, it is seen that although Specimens 18 and 24 have the same radius (3 mm) and very close values of strength, the experimental manufacturing parameters are quite different (30°/70% vs. 45°/50%). Such ambiguity causes the estimation inaccuracy for Specimen 5. Summarizing the above, the estimation result of FIS depends on the provided experimental data or fuzzy rules where ambiguous conformity could cause extra estimation error. Such ambiguity will be discussed in Section 4.

3.7 | Numerical validation

It can be seen from Table 3 that the two manufacturing parameters of interest can be estimated accurately. The average estimation error for manufacturing angle and infill density were seen to be 8.3° and 4.4%, respectively. At this stage, a validation test was designed in order to demonstrate the full capability and accuracy of FIS methodology. Authors appreciate the unconventional usage of the word "validation" in a numerical rather than traditionally experimental sense but offer readers to follow them.

In this numerical validation test, illustrated in Figure 3, we start from the inverse FIS (denoted F_1), in order to estimate manufacturing parameters (manufacturing angle and infill density) required to obtain the desired strength values and notch root radius. We follow the process described above in Sections 3.1–3.4. These obtained manufacturing parameters, after adjustments, discussed in Section 3.6, are then used together with the notch root radius in the next step—the direct FIS[26] (denoted F_2) to *(re-)estimate* values of the strength. Eventually, these new (re-)estimated values of the strength are compared to the original experimental failure strength values. The accuracy of the comparison will indicate whether FIS methodologies worked well.

As shown in Table 4, "manufacturing parameters" columns present the outcome of F_1. These data are
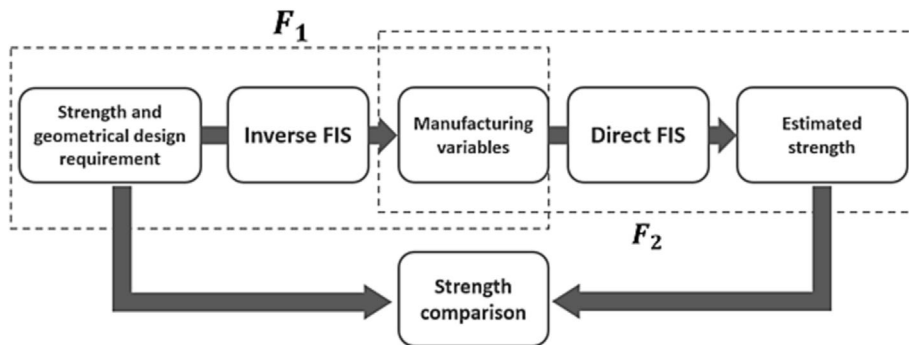

FIGURE 3 Explanation of inverse and direct estimation using FIS where F_1 refers to as inverse estimation and F_2 is the direct validation estimation.

TABLE 4 Estimated manufacturing angle and infill density are brought back into the FIS direct estimation to estimate the failure strength, which is to be compared with the experimental failure strength for $R = 1$ specimens.

Specimens ($R = 1$ mm)	Manufacturing parameters (adjusted)		Strength		Absolute error σ_f
	θ_p (°)	Infill (%)	Estimation σ_f (MPa)	Experimental σ_f (MPa)	
2	0	30	9.94	9.5	0.4
5	30	60	12.2	13.8	1.6
8	15	70	15.2	16.9	1.7
11	30	30	8.57	8.5	0.1
14	30	60	12.2	12.0	0.2
17	30	60	12.2	11.9	0.3
20	30	30	8.57	8.1	0.5
23	30	60	12.2	11.9	0.3
26	45	70	15.3	15.2	0.1
			Average error		0.6

then used in the new direct estimation FIS F_2, together with the radius in order to (re-)estimate failure strength (presented in "strength estimation" column). The new direct estimation still uses the aforementioned specimens to set up fuzzy rules, and the validation group is identical to that of inverse estimation. Estimated failure strength is then compared with experimental failure strength, and an absolute error is calculated. It can be seen (from Table 4) that the average absolute error

is 0.6 MPa, which is relatively small, compared to actual strength values. To reiterate, this error refers to the difference of failure strength obtained from experiments and estimated using our inverse-adjusted-direct approach. It is noted that at the end of the direct estimation process, the estimation error already includes errors generated in both inverse and direct FIS. Therefore, it can be concluded that FIS has proven to show a good performance.

TABLE 5 Inverse FIS estimation of manufacturing parameters with printing period and material weight being included.

	Input				Experiment output		Estimated adjusted output		Absolute error without time and weight (from Table 3)		Absolute error including time and weight	
No.	Radius (mm)	σ_f (MPa)	Print time (min)	Mat. weight (g)	θ_p (°)	Infill (%)	θ_p (°)	Infill (%)	ABS error θ_p	ABS error infill	ABS error θ_p	ABS error infill
1	0.5	9.7	93	8	0	30						
2	1	9.5	94	8	0	30	0	30	0	0	0	0
3	3	10.9	97	8	0	30						
4	0.5	13.1	101	9	0	50						
5	1	13.8	102	9	0	50	45	50	30	10	45	0
6	3	14.4	105	9	0	50						
7	0.5	17.4	109	10	0	70						
8	1	16.9	110	10	0	70	0	70	15	0	0	0
9	3	18.6	113	10	0	70						
10	0.5	8.2	93	8	30	30						
11	1	8.5	94	8	30	30	30	30	0	0	0	0
12	3	10.0	96	8	30	30						
13	0.5	11.5	101	9	30	50						
14	1	12.0	102	9	30	50	30	50	0	10	0	0
15	3	12.5	105	9	30	50						
16	0.5	12.2	109	10	30	70						
17	1	11.9	110	10	30	70	30	70	0	10	0	0
18	3	13.9	113	10	30	70						
19	0.5	8.0	92	8	45	30						
20	1	8.1	93	8	45	30	30	30	15	0	15	0
21	3	9.8	96	8	45	30						
22	0.5	11.0	100	9	45	50						
23	1	11.9	101	9	45	50	30	50	15	10	15	0
24	3	13.5	104	9	45	50						
25	0.5	15.1	108	10	45	70						
26	1	15.2	109	10	45	70	45	70	0	0	0	0
27	3	16.4	112	10	45	70						
							Average error		8.3	4.4	8.3	0

4 | EXTENSIVE STUDY OF COST-CONTROL RELEVANT PARAMETERS WITH FIS

In this section, we would like to return to the ambiguity issue, discussed in Section 3.7. It is noted that Specimen 23, for example, has 45°/50% experimental setup but the estimation result offers as preferred 30°/60% (see Table 3). The difference between both pairs cannot be disregarded; however, the 30°/60% provides a failure strength similar to 45°/50% (see Table 4). It can be referred to as the non-uniqueness of 3D-printing, that is, different combinations of multiple parameters can lead to similar results. Assuming there are no restrictions on manufacturing angles with respect to cost, this ambiguity of results can also be controlled by, for example, the material cost of the printing, where the solution with less infill density could be preferred (as discussed Section 1). Hence, it has risen extensive interest of authors that from the above inference process, parameters such as printing period and material consumption are worth of extra attention, especially for manufacturers.

Table 5 presents the study which includes not only strength and notch root radius but also printing period and material consumption for the estimation of optimal manufacturing parameters. Both printing period and material consumption have been acquired from the software CURA with different design models loaded, where the assumption has been made that the estimated time and material usage shown in CURA is identical to reality.[31] The printing period refers to the time (minutes) needed to complete the 3D-printing, while material consumption can quantify the weight of the material being consumed (grams). Both of them can be categorized as cost-relevant parameters which represent special industrial needs rather than manufacturing settings or geometrical design. Thus, they are used together with radius and strength as input of a new inverse FIS.

The setup of the new inverse FIS with two extra input parameters is similar to the one discussed in Section 3. Table 5 reports the new estimation error of recommended manufacturing angle is 8.3° (estimation *with* time and weight), which is identical to the outcome in Table 3 (estimation *without* time and weight). It is even more satisfying to see the new estimation error for infill density drops from 4.4% (without time and weight) to 0% (with time and weight). Such comparison leads to the following conclusions.

- Including additional parameters (such as printing time and material consumption) can lead to better FIS estimation accuracy for infill density while it has no significant impact on manufacturing angle.

- Generalizing further, it can be concluded that the manufacturing angle does not significantly influence the printing time and material consumption contrary to infill density.

Once again, the above result proves that FIS is a useful tool that can be used to estimate manufacturing angles and infill densities with not only requirements of failure strength and notch root radius but also cost-control parameters such as printing time and material consumption. Additional relevant parameters can contribute to better estimation accuracy using FIS.

5 | CONCLUSION

Following the present study, key steps of setting up a Sugeno FIS were discussed and demonstrated, together with parameter settings. Different from the previous work, here, FIS has shown its capability of estimating inversely, that is, estimating manufacturing angle and infill density with provided requirements of tensile strength and geometrical characteristic (notch root radius) in 3D-printing application. The necessity of having adjustments for estimation results has been discussed due to the specification of 3D-printers, and it has been shown that adjustments are effective and not resulting in an evident reduction of the estimation accuracy. It was concluded that FIS has a highly accurate inverse estimation potential.

Due to the intrinsic versatility of FIS, it has been demonstrated that during the inverse estimation, FIS is able to deal with a variety of parameters, including not only strength and geometry but also cost-relevant ones such as printing period and material consumption. It shows a comprehensive solution which allows manufacturers to find the optimal manufacturing parameters and have a cost-control tool at the same time.

Summarizing, FIS is able to offer high estimation accuracy as a robust and simple methodology. It has great potential of being an effective decision-making and cost-control tool in design problems for modern industries. It can be foreseen that FIS approach could be widely applied in engineering fields for mechanical behavior prediction, geometrical characteristics optimization, and industrial user needs.

DATA AVAILABILITY STATEMENT
The data that support the findings of this study are available from the corresponding author upon reasonable request.

NOMENCLATURE
R notch root radius

y_p	printing direction of 3D-printer
P_{est}	estimated parameter
P_{exp}	experimental parameter
θ_p	manufacturing angle of 3D-printing
μ	membership value of corresponding data
σ_f	tensile failure strength

ORCID

Luca Susmel 🄳 https://orcid.org/0000-0001-7753-9176

REFERENCES

1. Morimoto Y, Onoe H, Takeuchi S. Biohybrid robot powered by an antagonistic pair of skeletal muscle tissues. *Sci Robot*. 2018; 3(18):eaat4440.
2. Choi YJ, Kim TG, Jeong J, et al. 3D cell printing of functional skeletal muscle constructs using skeletal muscle-derived bioink. *Adv Healthc Mater*. 2016;5(20):2636-2645.
3. Dolati F, Yu Y, Zhang Y, Jesus AMD, Sander EA, Ozbolat IT. In vitro evaluation of carbon-nanotube-reinforced bioprintable vascular conduits. *Nanotechnology*. 2014;25(14): 145101.
4. Kolesky DB, Homan KA, Skylar-Scott MA, Lewis JA. Three-dimensional bioprinting of thick vascularized tissues. *Proc Natl Acad Sci U S A*. 2016;113(12):3179-3184.
5. Zhang B, Gao L, Ma L, Luo Y, Yang H, Cui Z. 3D bioprinting: a novel avenue for manufacturing tissues and organs. *Engineering*. 2019;5(4):777-794.
6. Wesemann C, Pieralli S, Fretwurst T, et al. 3-D printed protective equipment during COVID-19 pandemic. *Materials (Basel)*. 2020;13(8):1997.
7. Johnson AA, Bingham GA, Majewski CE. Laser sintered body armour: establishing guidelines for dual-layered stab protection. *Int J Rapid Manuf*. 2015;5(1):3-19.
8. General Electric. *What is Additive Manufacturing|GE Additive*. General Electric. Available at: https://www.ge.com/additive/additive-manufacturing; 2022. Accessed August 19, 2022.
9. Forés-Garriga A, Pérez MA, Gómez-Gras G, Reyes-Pozo G. Role of infill parameters on the mechanical performance and weight reduction of PEI Ultem processed by FFF. *Mater Des*. 2020;193:108810.
10. Tanveer MQ, Haleem A, Suhaib M. Effect of variable infill density on mechanical behaviour of 3-D printed PLA specimen: an experimental investigation. *SN Appl Sci*. 2019;1: 1701.
11. Porter JH, Cain TM, Fox SL, Harvey PS. Influence of infill properties on flexural rigidity of 3D-printed structural members. *Virtual Phys Prototyp*. 2019;14(2):148-159.
12. Birosz MT, Ledenyák D, Andó M. Effect of FDM infill patterns on mechanical properties. *Polym Test*. 2022;113:107654.
13. Podroužek J, Marcon M, Ninčević K, Wan-Wendner R. Bio-inspired 3D infill patterns for additive manufacturing and structural applications. *Materials (Basel)*. 2019;12(3):499.
14. Pernet B, Nagel JK, Zhang H. Compressive strength assessment of 3D printing infill patterns. In: *Procedia CIRP*. Vol.105. Elsevier; 2022:682-687.
15. Ganeshkumar S, Kumar SD, Magarajan U, et al. Investigation of tensile properties of different infill pattern structures of 3D-printed PLA polymers: analysis and validation using finite element analysis in ANSYS. *Materials (Basel)*. 2022;15(15):5142.
16. Dwiyati ST, Kholil A, Riyadi R, Putra SE. Influence of layer thickness and 3D printing direction on tensile properties of ABS material. *J Phys Conf Ser*. 2019;1402(6):066014.
17. Yousefi AA. Effects of 3D printer nozzle head temperature on the physical and mechanical properties of PLA based product. In: *Proceedings of the 12th International Seminar on Polymer Science and Technology*. Islamic Azad University; 2016:3-5.
18. Somireddy M, Czekanski A. Anisotropic material behavior of 3D printed composite structures—material extrusion additive manufacturing. *Mater Des*. 2020;195:108953.
19. Ziemian C, Sharma M, Ziemi S. Anisotropic mechanical properties of ABS parts fabricated by fused deposition modelling. In: *Mechanical Engineering*. IntechOpen; 2012:159-180.
20. Ezeh OH, Susmel L. Reference strength values to design against static and fatigue loading polylactide additively manufactured with in-fill level equal to 100%. *Mater Des Process Commun*. 2019;1(4):e45.
21. Nurizada A, Kirane K. Induced anisotropy in the fracturing behavior of 3D printed parts analyzed by the size effect method. *Eng Fract Mech*. 2020;239:107304.
22. Floor J, Van Deursen B, Tempelman E. Tensile strength of 3D printed materials: review and reassessment of test parameters. *Mater Test*. 2018;60(7–8):679-686.
23. Koch C, Van Hulle L, Rudolph N. Investigation of mechanical anisotropy of the fused filament fabrication process via customized tool path generation. *Addit Manuf*. 2017;16: 138-145.
24. Ng CT, Susmel L. Notch static strength of additively manufactured acrylonitrile butadiene styrene (ABS). *Addit Manuf*. 2020; 34:101212.
25. Hager I, Maroszek M, Mróz K, et al. Interlayer bond strength testing in 3D-printed mineral materials for construction applications. *Materials (Basel)*. 2022;15(12):4112.
26. Tu R, Gitman I, Susmel L. Fuzzy inference system for failure strength estimation of plain and notched 3D-printed polylactide components. *Fatigue Fract Eng Mater Struct*. 2022;45(6): 1663-1677.
27. Weake N, Pant M, Sheoran A, Haleem A, Kumar H. Optimising parameters of fused filament fabrication process to achieve optimum tensile strength using artificial neural network. *Evergreen*. 2020;7(3):373-381.
28. Kannan S, Vezhavendhan R, Kishore S, Kanumuru KV. Investigating the effect of orientation, infill density with Triple raster pattern on the tensile properties for 3D Printed samples. *IOP SciNotes*. 2020;1(2):024405.
29. Esakki B, Rajamani D, Arunkumar P. An intelligent modeling system to predict mechanical strength characteristics of selective inhibition sintered parts using fuzzy logic approach. *Mater Today Proc*. 2018;5(5):11727-11737.
30. Nawafleh N, AL-Oqla FM. An innovative fuzzy-inference system for predicting the mechanical behavior of 3D printing thermoset carbon fiber composite materials. *Int J Adv Manuf Technol*. 2022;121(11–12):7273-7286.
31. Ahmed AA, Susmel L. Static assessment of plain/notched polylactide (PLA) 3D-printed with different infill levels: equivalent homogenised material concept and Theory of

Critical Distances. *Fatigue Fract Eng Mater Struct.* 2019; 42(4):883-904.

32. Zadeh LA. Fuzzy sets. *Infect Control.* 1965;8(3):338-353.

33. Ross TJ. *Fuzzy Logic with Engineering Applications.* 3rd ed. John Wiley & Sons; 2010.

34. Zimmermann HJ. Fuzzy set theory. *Wiley Interdiscip Rev Comput Stat.* 2010;2(3):317-332.

35. Kalogirou SA. Designing and modeling solar energy systems. In: *Solar Energy Engineering.* Academic Press; 2009: 553-664.

36. Guillaume S. Designing fuzzy inference systems from data: An interpretability-oriented review. *IEEE Trans Fuzzy Syst.* 2001; 9(3):426-443.

37. Sugeno M. *Industrial Applications of Fuzzy Control.* North-Holland; 1985.

38. Mamdani EH, Assilian S. An experiment in linguistic synthesis with a fuzzy logic controller. *Int J Man Mach Stud.* 1975;7(1): 1-13.

39. Princy S, Dhenakaran SS. Comparison of triangular and trapezoidal fuzzy membership function. *J Comput Sci Eng.* 2016;2: 46-51.

40. Zhao J, Bose BK. Evaluation of membership functions for fuzzy logic controlled induction motor drive. *IECON Proc (Industrial Electron Conf).* 2002;1:229-234.

41. Adil O, Ali A, Ali M, Ali AY, Sumait BS. Comparison between the effects of different types of membership functions on fuzzy logic controller performance. *Int J Emerg Eng Res Technol.* 2015;3:76-83.